General Disclaimer

One or more of the Following Statements may affect this Document

- This document has been reproduced from the best copy furnished by the organizational source. It is being released in the interest of making available as much information as possible.

- This document may contain data, which exceeds the sheet parameters. It was furnished in this condition by the organizational source and is the best copy available.

- This document may contain tone-on-tone or color graphs, charts and/or pictures, which have been reproduced in black and white.

- This document is paginated as submitted by the original source.

- Portions of this document are not fully legible due to the historical nature of some of the material. However, it is the best reproduction available from the original submission.

Produced by the NASA Center for Aerospace Information (CASI)

NATIONAL AERONAUTICS AND SPACE ADMINISTRATION

Technical Memorandum 33-748

Performance of a Solar-Thermal Collector

W. H. Higa

JET PROPULSION LABORATORY

CALIFORNIA INSTITUTE OF TECHNOLOGY

PASADENA, CALIFORNIA

November 1, 1975

Technical Memorandum 33-748

Performance of a Solar-Thermal Collector

W. H. Higa

1. Report No. 33-748	2. Government Accession No.	3. Recipient's Catalog No.

4. Title and Subtitle	5. Report Date
PERFORMANCE OF A SOLAR-THERMAL COLLECTOR	November 1, 1975
	6. Performing Organization Code

7. Author(s) W. H. Higa	8. Performing Organization Report No.

9. Performing Organization Name and Address	10. Work Unit No.
JET PROPULSION LABORATORY California Institute of Technology 4800 Oak Grove Drive Pasadena, California 91103	11. Contract or Grant No. NAS 7-100
	13. Type of Report and Period Covered

12. Sponsoring Agency Name and Address	Technical Memorandum
NATIONAL AERONAUTICS AND SPACE ADMINISTRATION Washington, D.C. 20546	14. Sponsoring Agency Code

15. Supplementary Notes

16. Abstract

Many evolutionary steps are required before a solar-thermal power system can be moved from the research laboratory phase to the field applications area. It is the objective of this paper to discuss some possible means for achieving the required technology. Simplifications in construction techniques as well as in measurement techniques for parabolic trough collectors are described. Actual measurement data is also given.

17. Key Words (Selected by Author(s))	18. Distribution Statement
Fluid Mechanics and Heat Transfer Mechanical Engineering Energy Production and Conversion Thermodynamics and Statistical Physics	Unclassified -- Unlimited

19. Security Classif. (of this report)	20. Security Classif. (of this page)	21. No. of Pages	22. Price
Unclassified	Unclassified	20	

HOW TO FILL OUT THE TECHNICAL REPORT STANDARD TITLE PAGE

Make items 1, 4, 5, 9, 12, and 13 agree with the corresponding information on the report cover. Use all capital letters for title (item 4). Leave items 2, 6, and 14 blank. Complete the remaining items as follows:

3. Recipient's Catalog No. Reserved for use by report recipients.

7. Author(s). Include corresponding information from the report cover. In addition, list the affiliation of an author if it differs from that of the performing organization.

8. Performing Organization Report No. Insert if performing organization wishes to assign this number.

10. Work Unit No. Use the agency-wide code (for example, 923-50-10-06-72), which uniquely identifies the work unit under which the work was authorized. Non-NASA performing organizations will leave this blank.

11. Insert the number of the contract or grant under which the report was prepared.

15. Supplementary Notes. Enter information not included elsewhere but useful, such as: Prepared in cooperation with... Translation of (or by)... Presented at conference of... To be published in...

16. Abstract. Include a brief (not to exceed 200 words) factual summary of the most significant information contained in the report. If possible, the abstract of a classified report should be unclassified. If the report contains a significant bibliography or literature survey, mention it here.

17. Key Words. Insert terms or short phrases selected by the author that identify the principal subjects covered in the report, and that are sufficiently specific and precise to be used for cataloging.

18. Distribution Statement. Enter one of the authorized statements used to denote releasability to the public or a limitation on dissemination for reasons other than security of defense information. Authorized statements are "Unclassified—Unlimited, " "U.S. Government and Contractors only, " "U.S. Government Agencies only, " and "NASA and NASA Contractors only. "

19. Security Classification (of report). NOTE: Reports carrying a security classification will require additional markings giving security and down-grading information as specified by the Security Requirements Checklist and the DoD Industrial Security Manual (DoD 5220.22-M).

20. Security Classification (of this page). NOTE: Because this page may be used in preparing announcements, bibliographies, and data banks, it should be unclassified if possible. If a classification is required, indicate separately the classification of the title and the abstract by following these items with either "(U)" for unclassified, or "(C)" or "(S)" as applicable for classified items.

21. No. of Pages. Insert the number of pages.

22. Price. Insert the price set by the Clearinghouse for Federal Scientific and Technical Information or the Government Printing Office, if known.

PREFACE

The work described in this report was performed by the
Telecommunications Division of the Jet Propulsion Laboratory.

ACKNOWLEDGMENT

CONTENTS

TABLE

FIGURES

ABSTRACT

Many evolutionary steps are required before a solar-thermal power
system can be moved from the research laboratory phase to the field
applications area. It is the objective of this paper to discuss some
possible means for achieving the required technology. Simplifications
in construction techniques as well as in measurement techniques for
parabolic trough collectors are described. Actual measurement data
is also given.

I. INTRODUCTION

The objective of this paper is to study the performance of a parabolic trough solar-thermal collector with axis oriented parallel to the N-S Earth axis. The emphasis is on simplified experimental techniques to provide rapid evaluation of a collector system. A brief description of a simple parabolic collector is given in Section II. In Section III a simple method for determining the thermal losses in a receiver pipe is described.

An analytical formulation for the direct component of insolation on a clear day is given in Section IV in preparation for the actual determination of the performance of a solar-thermal collector, which is given in Section V. In Section VI actual experimental data is analyzed by the methods developed in the paper.

II. PARABOLIC COLLECTOR DESIGN

The basic approach in the fabrication of a parabolic collector was to machine parabolic ribs in a programmed milling machine; these ribs were then attached to a torque tube as shown in Figure 1. Aluminum sheets 3.2 mm (1/8 in.) thick were then rolled to the appropriate circular radius to match the parabolic shape of the ribs. The preformed aluminum sheets were then bolted on to the ribs to serve as the foundation for the parabolic collector. The mirror (not shown) was a 3.2-mm (1/8-in.)-thick sheet of acrylic aluminized on one side (Ram Products: Industrial grade mirror) and was clamped into the structure in a simple manner for easy replacement. The aluminized acrylic mirror had a reflectivity of around 85% even though the radiation had to traverse the plastic twice. The protection of the mirror by the plastic is a desirable feature for hostile environments and well worth the small sacrifice in reflectivity.

The drive mechanism was not a matter of concern in this investigation, and a synchronous motor with a gear box was used in conjunction with a chain drive to provide adequate solar tracking. The techniques used profited from the experiences of the Minneapolis-Honeywell project[1]*, and the author is grateful to Dr. J. Ramsey for helpful information.

The primary objective of this project was to develop measurement techniques, and the collector was designed to facilitate these measurements. No effort was made to optimize the fabrication procedure described. Even so, the performance of the collector met all expectations as will be described.

III. DETERMINATION OF THERMAL LOSSES

A simple way to determine the thermal losses in a solar-thermal collector is shown in Figure 2. A thin-walled stainless steel tube is treated with the appropriate selective coating and mounted as shown. A high-current low-voltage power transformer is then used to heat the tube. After temperature equilibrium is reached, the thermal loss is measured directly by measuring the electrical power being supplied. Thermocouples are placed inside the tube at a few places to ensure that uniform equilibrium temperature has been achieved; this is necessary to ensure that no longitudinal heat flow is occurring. Figure 3 shows a typical set of curves for a 2.5-cm stainless steel tube prior to application of any coating. Figure 4 is a photograph of the experimental arrangement used.

Lest one dismisses the measurement as being trivial, it should be pointed out that the measurement of the effective infra-red emissivity of a selectively coated surface is not an easy task. With the technique described here it is

---

*Numerals in parenthesis refer to references cited at end of paper.

only necessary to evacuate the enclosing glass tube and to know the emissivity of the glass[2] for the corresponding temperature. One can then compute the emissivity sought. Another difficult measurement which can be performed quite easily with the apparatus described is the behavior of convection loss as a function of tilt angle relative to the horizontal position. It should be appreciated that these measurements are difficult to perform once the collector pipe is mounted on the parabolic collector assembly.

Finally, it is necessary to point out that there will be a small difference in the thermal properties of the collector pipe as measured here compared with the actual installed pipe. Here the temperature is uniform in the circumferential direction at any given location of the pipe. In the installed pipe, the temperature on the side where the sunlight is focussed may be higher than on the opposite side. However, the temperature difference is not large enough to yield serious errors.

IV. ANALYTICAL REPRESENTATION OF INSOLATION

In preparation for the measurement of the performance of a solar energy collector, it is desirable to derive a simple analytical expression for the clear day insolation. For concentrating collectors only the direct normal component of the radiation is of importance.

The mathematical expression for the direct normal solar intensity as given in the ASHRAE Handbook of Fundamentals[3] is compact but cumbersome for calculations. In addition it is inaccurate at sunrise and sunset. This becomes obvious when one plots

$$I_{DN} = A \exp(-B/\sin b) \qquad (1)$$

where

A = apparent solar irradiation at (at air mass = 0)

B = atmospheric extinction coefficient

and

$$\sin b = \cos L \cos \delta \, \cos H + \sin L \sin \delta$$

here   L = local latitude

        δ = solar declination

        H = hour angle = (1/4) x no. min from local solar noon.

Equation (1) is based on a flat Earth-atmosphere approximation, and is at least useful over the important part of the day. A more accurate representation is easily derivable for a uniform, concentric, spherical atmosphere of finite thickness. This is given by

$$I_{DN} = A \exp (-B'S) \qquad (2)$$

where

$$S = R \left[\frac{h}{R} + \sqrt{1 + \frac{2h}{R} \cot^2 \theta} - 1 \right] \sin\theta \qquad (3)$$

A = same as ASHRAE

R = Earth's radius (6400 km (4000 mi))

h = thickness of a uniform atmosphere (32 km (20 mi))

θ = solar angle measured from local horizon

and

$$B'h = ASHRAE \, B$$

Unfortunately, even if Eq. (2) is more accurate than Eq. (1), it is evident that neither are suitable for computational purposes. Fortunately, a simple expression can be used as a good approximation to Eq. (2). This is given by

$$I_{DN} = A' \left[1 - \exp (-B'' \theta) \right]$$
$$0 < \theta < \frac{\pi}{2} \quad \text{mornings}$$
$$I_{DN} = A' \left[1 - \exp \left(-B'' (\pi - \theta) \right) \right] \qquad (4)$$
$$\frac{\pi}{2} < \theta < \pi \quad \text{afternoons}$$

where the constants A' and B'' are adjusted to match the data on insolation. Figure 5 is an actual recording from a tracking heliometer and shows that the direct-normal component of insolation is indeed well represented by Eq. (4). In Equation (4) the angle θ is given by

$$\theta = \omega_o t \qquad \qquad (5)$$

where ω_o is the Earth's rotational rate which is, of course, a seasonal variable.

Equation (4) will be used in calculating the performance of a solar energy collector. The utility of Eq. (4) may be illustrated, for example, in computing the total solar energy available per annum. This is given by

$$W = 2 \sum_{n=1}^{360} \int A_n' \left[1 - e^{-B_n'' \omega_n t_n} \right] dt_n \qquad (6)$$

where $\qquad A_n' \cong A_o + a_o \cos n \qquad \qquad (7)$

where the constants A_o and a_o may be computed from ASHRAE data, and n is the day number in degrees with Dec. 21 taken as day zero and day 360. (The fact that there are really 365 days per year is a minor defect in the Earth's orbital motion which we overlook in the interest of computational elegance.) Similarly, B'' is given by

$$B'' \cong B_o - b_o \cos n \qquad \qquad (8)$$

Again the constants B_o and b_o may be computed from ASHRAE. The calculations for ω_n and t_n are likewise very simple. Figure 6 shows a plot of the ASHRAE constants A, B, and δ, the tilt angle of the Earth.

The integration in Eq. (6) is easy; this is not the case for either expression in Eq. (1) or (2).

V. SOLAR COLLECTOR EVALUATION

The performance of solar energy collectors may be determined through some simple calorimetric measurements. By supplementing experimental data with reasonable approximations it is possible to derive a theoretical model which permits the calculation of the performance under various operating conditions.

The analyses described here are particularly adapted to cylindrical trough collectors. As stated previously the detailed design and fabrication of solar collectors have been discussed in considerable detail in the literature (Refs. 1, 4). The purpose here is to consider the evaluation of the performance of a given solar-thermal system. A simplified calorimetric procedure is suggested as shown in Figure 7. Instead of using the usual flowing fluid for measurements, a solid rod of metal, such as aluminum, is used for calorimetry.

The thermal balance equation for Figure 7 is given by

$$I_0 A_e \eta_0 \cos \phi = MC \frac{dT}{dt} + K_1 \left(T^4 - T_a^4 \right) + K_2 \left(T - T_a \right) \tag{9}$$

where

I_0 = direct normal insolation

A_e = effective area of solar collector per unit length

η_0 = optical efficiency

M = mass of Al rod

C = specific heat of Al rod

ϕ = solar angle (see Figure 7)

T = temp of od in Kelvins

T_a = ambient temperature

K_1 = radiation loss parameter

K_2 = convection loss parameter (in linear approximation)

The motivation for the present approach is the observation that the insolation is substantially constant between 10 a.m. and 2 p.m. on a clear day. For a polar-mounted collector, the solar angle, $\emptyset$, is also constant; hence, the input is an easily measured constant for any given clear day. Under these circumstances the non-linear heat balance equation may be solved in various approximations as discussed below.

A. THE LINEAR APPROXIMATION

It is well known that for small variations in temperature the radiation loss term in Eq. (9) may be approximated as

$$K_1 \left(T_o^2 + T_a^2 \right) \left(T_o + T_a \right) \left(T - T_a \right) \tag{10}$$

where T_o is the mean operating temperature. Thus for small variations in T about T_o, the radiation loss (10) may be combined with the linear loss term in Eq.(9) or

$$I(t) = MC \frac{dT}{dt} + K (T - T_a) \tag{11}$$

where K is a new constant which accounts for all losses and

$$I(t) = I_o A_e \eta_o \cos \emptyset$$

Although Eq. (11) is applicable for a relatively small temperature range, it is exactly solvable even for the case when insolation I(t) is a variable (cloudy day). Some insight into the dynamics of a solar collector could thus be gained.

B. NON-LINEAR APPROXIMATION

An alternative approximation to Eq. (9) is to assume dominance of the radiation loss term; then

$$I(t) = MC \frac{dT}{dt} + K_0 \left(T^4 - T_a^4 \right) \qquad (12)$$

where K_0 is adjusted to account for all thermal losses. Eq. (12) is applicable especially to high-temperature operation of a collector. Figure 8 shows a typical heating curve for constant insolation. The first deduction from Figure 8 and Eq. (12) is that initially there are no losses because $T = T_a$. Thus

$$MC \left(\frac{dT}{dt} \right)_0 = I_0 A_e \eta_0 \cos \emptyset \qquad (13)$$

where $(dT/dt)_0$ indicates the initial slope at $t = 0$. All quantities in Eq. (13) are known except η_0, the optical efficiency, which is given by

$$\eta_0 = \rho\tau\alpha = MC \left(\frac{dT}{dt} \right)_0 \bigg/ I_0 A_e \cos \emptyset \qquad (14)$$

here

      ρ = mean reflectivity of mirror

      τ = mean transmissivity of glass tube (see Figure 7)

      α = mean absorptivity of pipe

The second observation from Figure 8 and Eq. (12) is that when thermal equilibrium is achieved, all the solar power incident on the receiver pipe is reradiated as infrared power and

$$K_o = I_o A_e \eta_o \cos \phi \Big/ \left(T_s^4 - T_a^4 \right) \qquad (15)$$

where K_o is the hitherto unknown loss parameter, and T_s is the stagnation temperature. All quantities in Eq. (12) are now known, and for any operating temperature, T_o, the thermal power available is given by

$$P_t(T_o) = MC \left(\frac{dT}{dt} \right)_{T=T_o} = I_o A_e \eta_o \cos \phi - K_o \left(T_o^4 - T_a^4 \right) \qquad (16)$$

In these equations it is to be noted that T_a really stands for the apparent ambient temperature. Unfortunately this effective temperature is not directly measurable. It is a function of the ambient temperature and the temperature of the glass tube, which varies from point to point. The infra-red properties of the glass finally provide the weighting function to be used with the above two temperatures.

One way to obtain, experimentally, a mean value for T_a is to record the cooling curve as well as the heating curve. This is simply achieved by turning the solar collector 180 degrees away from the sun after the rod has reached stagnation temperature.

The interesting information in the temperature vs. time recording is, of course, in the high-temperature region. Equation (12) is exactly solvable for high temperatures, and the solutions are, for heating and cooling, respectively

$$T = T_s \tanh \left[\frac{2K_o T_s^3 t}{MC} + \tanh^{-1} \frac{T_a}{T_s} \right], \qquad (17)$$

and

$$T = T_a \coth \left[\frac{2K_o T_a^3 t'}{MC} + \coth^{-1} \frac{T_s}{T_a} \right]. \qquad (18)$$

The time t' for the cooling curve should, of course, start at zero when $T = T_s$ at which time the collector is turned away from the sun.

Summarizing this lengthy discussion, it is observed that the heating and cooling curves are used with Eqs. (15), (17), and (18) to derive values for K_0 and T_a such that the curves are well matched by Eqs. (17) and (18) at least for the higher temperatures. Then Eq. (16) may be used to compute the available thermal power at any temperature. An actual recording from an experiment will be analyzed in detail in the next section to illustrate the procedure.

In the discussion of the linear approximation it was pointed out that Eq. (14) was exactly solvable even when the insolation varied with time. The present discussion concludes with the observation that Eq. (15) is solvable, in the high-temperature approximation, by rewriting it in the approximate form

$$I(t) = MC \frac{dT}{dt} + aK_0 \bar{T}^2 \left(T^2 - T_a^2 \right) \tag{19}$$

where $\bar{T}$ is the mean collector temperature. Eq. (19) is reducible to the standard Ricatti form and is solvable by standard methods even when the insolation varies with time.

VI. EXPERIMENTAL RESULTS

Figure 9 shows an actual heating and cooling curve obtained on a hazy day. The important parameters were as follows:

Date: June 24, 1975

Site: JPL, Pasadena, Ca.

I_0 = Average Insolation: 740 watts/m^2
10 a.m. to 2 p.m.

A_e = 2.3 m^2 = effective area of reflector

cos $\emptyset$ = .92

$$T_g = 120^\circ C \text{ (approximate glass temperature)}$$

$$T_a = 30^\circ C$$

$$C = \text{Sp. heat of Al} = .25 \text{ Cal/gm } ^\circ C$$

$$L = 2.3 \text{ m} = \text{length of Al rod}$$

$$d = 3.8 \text{ cm} = \text{diam. of Al rod}$$

$$M = 7000 \text{ gms.}$$

The calculations proceed very simply as follows:

(a) The total radiation impinging on the reflector surface is

$$I_o A_e \cos \emptyset = 1566 \text{ w.}$$

The net power which is converted to heating the rod is found by measuring the initial slope $(\Delta T/\Delta t)_o$ in the recording:

$$P_t = MC \left(\frac{\Delta T}{\Delta t} \right)_{t=0} = 1018 \text{ watts}$$

This gives the optical efficiency η_o for the collector as

$$\eta_o = \frac{P_t}{I_o A_e \cos \emptyset} = \frac{1018}{1566} = 65\%$$

Similarly, the available thermal power for any temperature T_o is found from the recording by measuring the slope $(\Delta T/\Delta t)_{T=T_o}$ or

$$P_t(T_o) = MC \left(\frac{\Delta T}{\Delta t} \right)_{T=T_o}$$

Alternatively, it is possible to use Eq. (16) by first computing the value for K_o by use of Eq. (15)

$$K_0 = \frac{I_0 A_e \eta_0 \cos \emptyset}{T_s^4 - T_a^4} = \frac{1018}{673^4 - 303^4} = 5.1 \times 10^{-9}$$

Note that if T_s is significantly higher than T_a, the constant K_0 is not too sensitive to errors in T_a. Table 1 shows values for P_t as calculated by the two methods described. It is noted that for greater accuracy the effective ambient temperature ought to be treated as a variable, but the added complexity would not warrant the exercise.

Figure 10 shows the available thermal power for the two operating temperatures used in the preceding examples. The choice of $230^\circ C$ as a possible working temperature for steam was selected as a reasonably low temperature while providing a high enough pressure for use with a steam turbine.

Finally, Figure 11a shows a drift curve for the collector. This curve is derived as follows: the parabolic collector is fixed in position near solar noon; the sun is then allowed to drift through the focusing position to provide the heating curve of Figure 11a. As a rough approximation the energy impinging on the rod is given by

$$I(t) = I_0 A_e \eta_0 \cos \emptyset \sin \omega t \tag{20}$$

where ωt is the angular drift rate of the sun (15° per hour). Since the temperature of the collector system doesn't get very high, the rate of heating of the rod is given by:

$$\frac{dT}{dt} = \frac{I_0}{MC} A_e \eta_0 \cos \emptyset \sin \omega t \tag{21}$$

Therefore the temperature as a function of time is

$$T = -T_{max} \cos \omega t \tag{22}$$

where T_{max} is the maximum temperature in Figure 11a. From Eq. (22) it is seen that the derivative of the drift curve gives the sinusoidal response of Eq. (21)

and is shown in Figure 11b. The width at the half power points is a rough measure of the accuracy required from the solar tracking mechanism. Here it is seen to be ± 1.5 degrees.

VII. CONCLUSIONS

The real significance of this investigation is that a solar-thermal collector has been used as an analog computer to solve a difficult heat transfer problem. The rigorous solution of the heat balance equations, which treat the effective ambient temperature as a variable, is not too important because the collector system analyzed is only an approximation to the real working system.

The emphasis here has been to treat the collector as a unit and to derive reasonably accurate measurement techniques. The details of mirror surface tolerances, receiver pipe coatings, antireflective surfaces for the glass tube, etc., have been discussed elsewhere in great detail and are not repeated here.

At the time when the experiment was performed to obtain Figure 9, it was realized that the black chrome surface could be damaged by the high temperature of 400°C which had been achieved. Subsequently during attempts to repeat the experiment to obtain comparative data, for example, for the no vacuum mode of operation, it was noticed that considerable deterioration had occurred to the black chrome.

REFERENCES

1. <u>Research Applied to Solar-Thermal Power Systems</u>, Report NSF/RANN/SE/
   G1-34871/PR/73/2, University of Minnesota and Honeywell.

2. Gardon, R., "The Emissivity of Transparent Materials," Journal of the
   American Ceramic Society, Vol. 39, No. 8, Aug. 1956.

3. <u>Handbook of Fundamentals</u>, American Society of Heating, Refrigerating,
   and Air-Conditioning Engineers (ASHRAE), G. Banta Publishing Co., Menasha,
   Wisconsin.

4. Duffie, J. A., and Beckman, W. A., <u>Solar Energy Thermal Processes</u>,
   J. Wiley & Sons, New York, 1974.

Table 1. Available thermal power at two operating temperatures as calcu-
lated from graph of Figure 9 compared with calculated values
from Eq. (16). The effective ambient temperature is an unknown
quantity somewhere between 30° and 120°C.

Available power	Calculated from Fig. 9	Calculated from Eq. (16)		
		$T_a = 30°C$	$T_a = 60°C$	$T_a = 90°C$
$P_t(230°C)$	733 W	728 W	749 W	776 W
$P_t(300°C)$	554 W	500 W	521 W	548 W
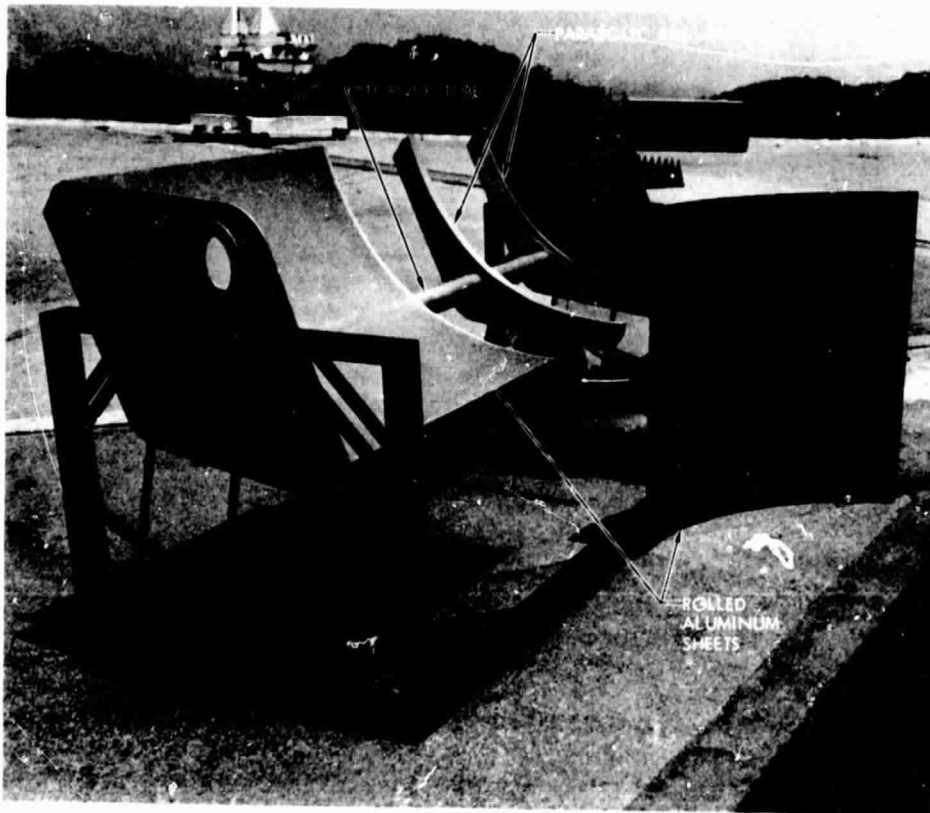
Fig. 1. Constructional details for a parabolic collector
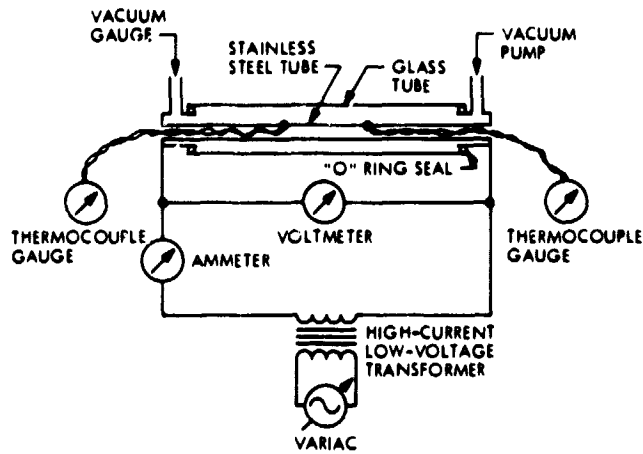
Fig. 2. Method for measuring thermal
losses in a solar-thermal collector
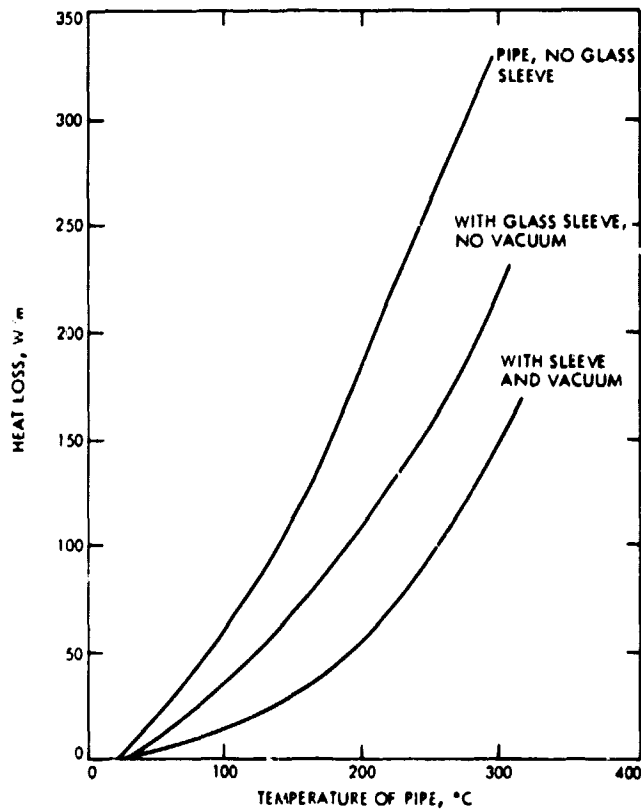
Fig. 3. Typical thermal loss curves for a
stainless steel pipe without surface
treatment (heat loss per unit length of
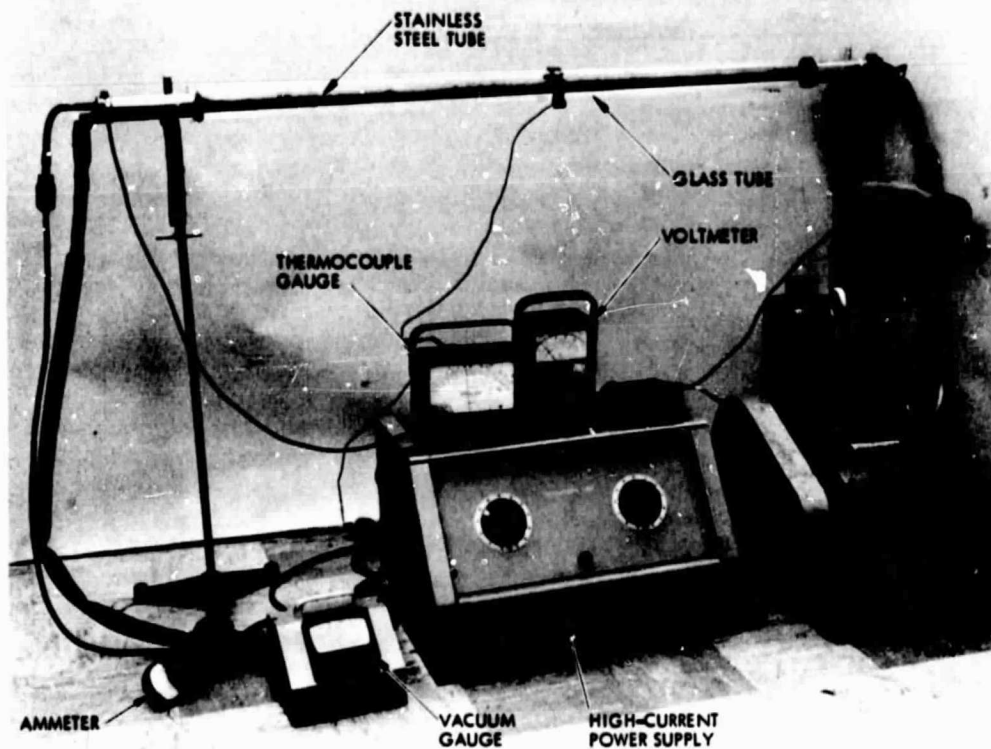2.5-cm-diam stainless steel pipe)

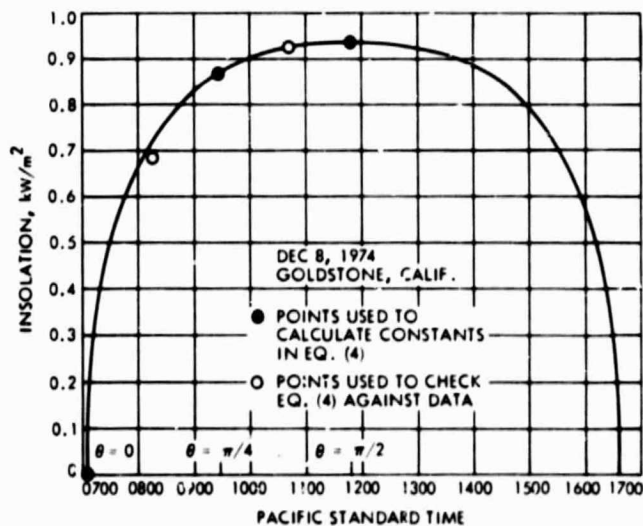Fig. 4. Experimental arrangement for measuring heat losses in a collector pipe

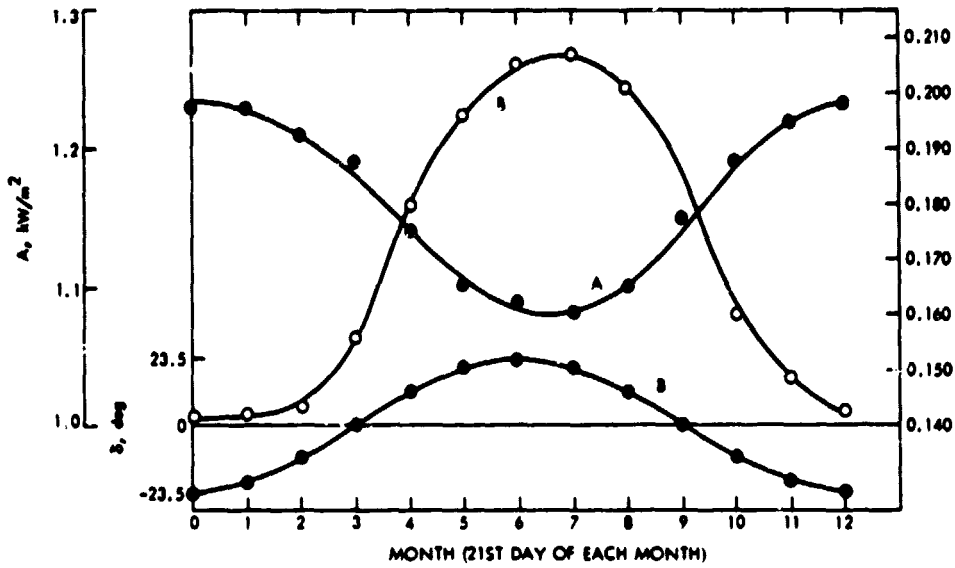Fig. 5. Typical clear day direct normal insolation at Goldstone, California

Fig. 6. Plot of ASHRAE constant A, B, φ (Note that A has been converted to kW/m^2)
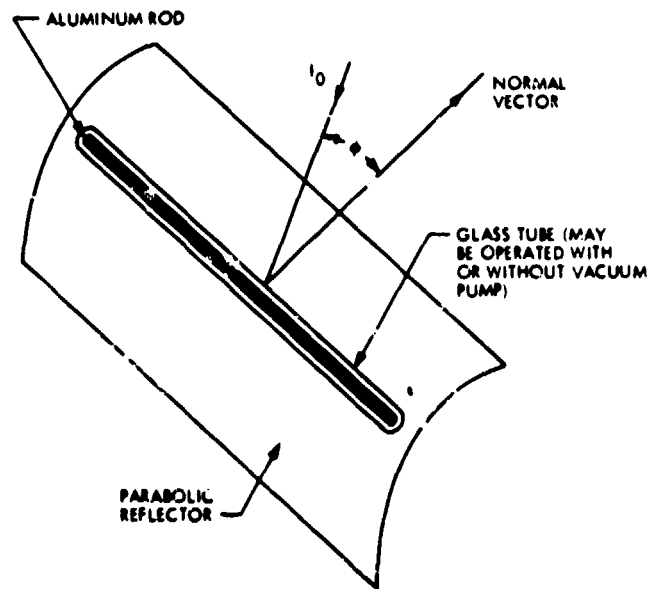
Fig. 7. Test arrangement for a solar-thermal collector
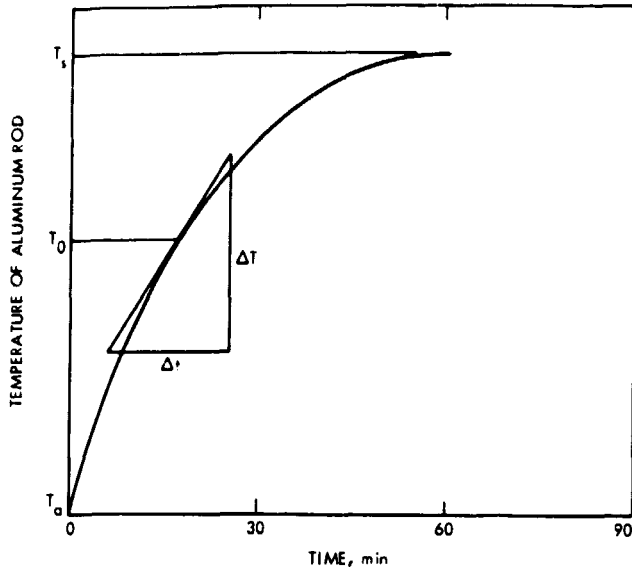
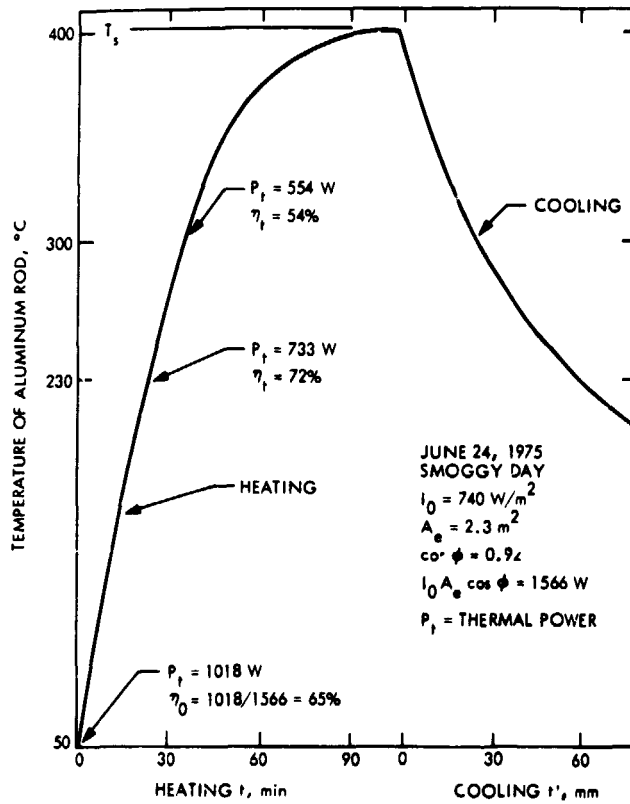Fig. 8. Hypothetical heating curve for arrangement of Figure 7

Fig. 9. Heating-cooling curves for Al rod coated with Harshaw Chemical "black chrome"
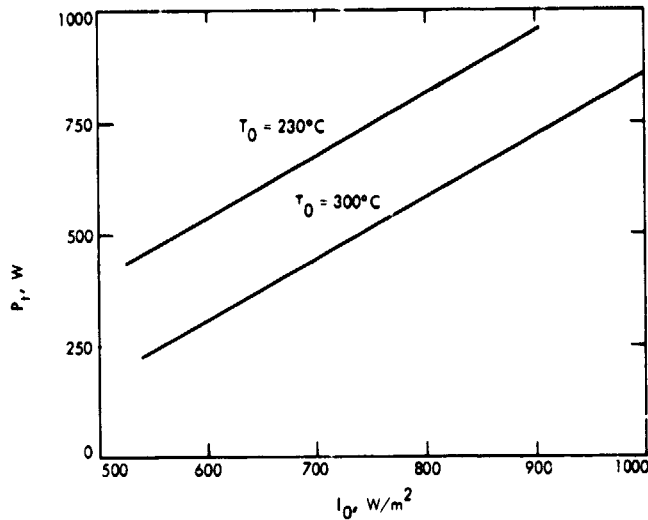
Fig. 10. Available thermal power as a
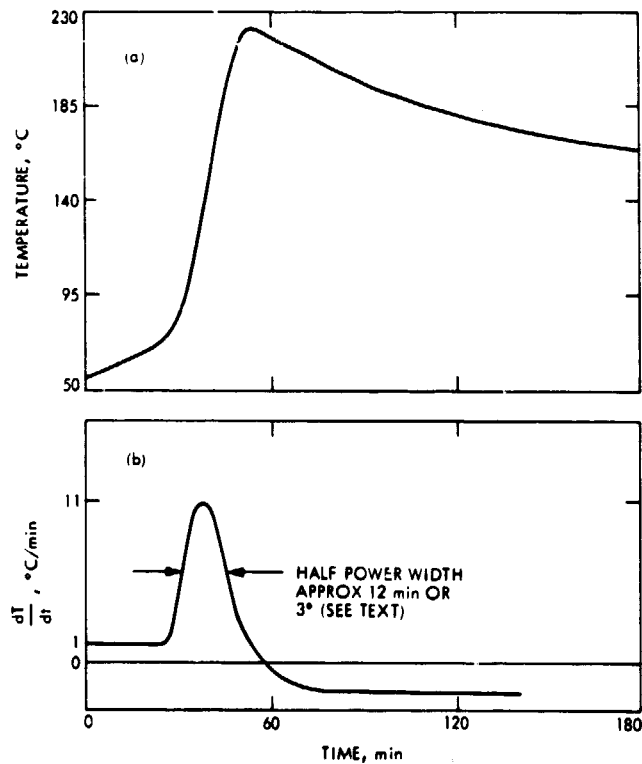function of insolation calculated from
Eq. (16)

Fig. 11. (a) Solar drift curve (see text);
(b) derivative of drift curve for deter-
mining tracking accuracy required (executed
freehand to illustrate a procedure)

JPL Technical Memorandum 33-748